Workshop 3: Flutter tests and Controllers

Aeroservoelasticity 2024/2025 - Prof. Quaranta

Team members	Personal code
Matteo Baio	10667431
Gaia Lapucci	10710434
Lorenzo Lucatello	10735694

Introduction

The aim of this workshop is evaluate the flutter characteristics of the XV-15 tiltrotor, evaluating the combined dynamics of the airframe and rotor. The first tasks required to implement the model of the aileron and rotor actuators, that are then used as means of exiting the system to execute flutter tests.

Input Data

The rotor data and model were the same as the ones used in the previous workshop. For the airframe instead, we were given a finite element model defined by 48 nodes and the respective connectivity elements. The modal mass matrix $\mathbf{M}_{hh}$, the modal damping matrix $\mathbf{C}_{hh}$, the modal stiffness matrix $\mathbf{K}_{hh}$ and the eigenvectors, as well as the aerodynamic matrices for the state space formulation were also given. The geometrical data of the prop-rotor is available in Table 1.

Radius	3.5 m
N. of blades	3
Solidity	0.10
NR	740 rpm

Table 1: Rotor data

Task 0: Load the rotor-airframe model

This task was straightforward and only required to load the combined model of the airframe and rotor that was developed in the previous workshop.

Task 1: Adding aileron actuators

Firstly, we need to establish the behavior of the actuator. Specifically, the actuator deforms in response to the applied force, due to its stiffness, and to the commanded input. The commanded input determines the deformation through a transfer function, which in this case corresponds to the one of a second-order system. Consequently, the dynamics of the aileron actuator can be described by the following equation:

$$\delta = -\frac{1}{K_{act}}F + \frac{\omega_n^2}{s^2 + 2\xi\omega_n s + \omega_n^2}\delta_c$$

The actuator stiffness is imposed to be $K_{act} = 9800 ^{Nm}/_{rad}$, the natural frequency is $\omega_n = 2\pi \cdot 12 ^{rad}/_{s}$ and the damping ratio has a unitary value (critical damping $\xi = 1$). As follows in Figure 1 we find the corresponding Bode plot of the transfer function associated with the aileron actuator dynamics.

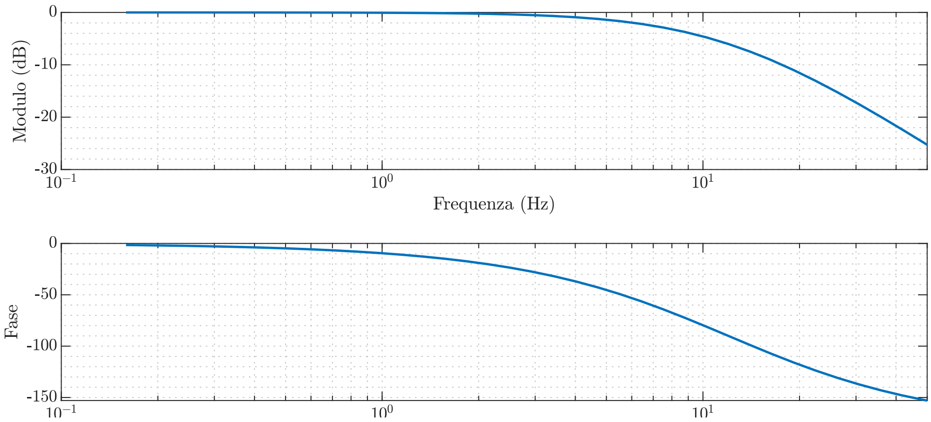

Figure 1: Bode plot of the actuator dynamics

To implement the actuator dynamics inside the system, we have to substitute the forcing term of the system dynamics equation with the actuator force. Therefore, by first calling:

$$\delta_0 = \frac{\omega_n^2}{s^2 + 2\xi\omega_n s + \omega_n^2}\delta_c$$

Then:

$$\delta = -\frac{1}{K_{act}}F + \delta_0 \quad \Rightarrow \quad F = -K_{act}(\delta - \delta_0)$$

At this point we can proceed with the substitution of the forcing term in the system dynamics equation. Recalling that the actuator stiffness acts on a specific degree of freedom of a specific node and because the matrices are in modal coordinates, we have to project the force as well into modal coordinates.

$$\mathbf{M}_A\ddot{\mathbf{q}}_a + \mathbf{C}_A\dot{\mathbf{q}}_a + \mathbf{K}_A\mathbf{q}_a = \mathbf{f} = \mathbf{\Phi}_A^T \begin{bmatrix} 0 \\ \vdots \\ F \\ \vdots \\ 0 \end{bmatrix} = -\mathbf{\Phi}_A^T \begin{bmatrix} 0 \\ \vdots \\ 1 \\ \vdots \\ 0 \end{bmatrix} K_{act}\,\delta + \mathbf{\Phi}_A^T \begin{bmatrix} 0 \\ \vdots \\ 1 \\ \vdots \\ 0 \end{bmatrix} K_{act}\,\delta_0$$

The aileron deflection δ can be expressed in terms of modal coordinate, therefore by carrying out such substitution, we can write the final equation:

$$\mathbf{M}_A\ddot{\mathbf{q}}_a + \mathbf{C}_A\dot{\mathbf{q}}_a + \left[\mathbf{K}_A + \mathbf{\Phi}_A^T \begin{bmatrix} 0 \\ \vdots \\ 1 \\ \vdots \\ 0 \end{bmatrix} K_{act}[0 \cdots 1 \cdots 0]\mathbf{\Phi}_A\right]\mathbf{q}_a - \mathbf{\Phi}_A^T \begin{bmatrix} 0 \\ \vdots \\ 1 \\ \vdots \\ 0 \end{bmatrix} K_{act}\,\delta_0 = \mathbf{0}$$

Recalling that the term δ_0 is determined by the actuator dynamics given the input δ_c, we can build the following system of equation which fully defines the dynamics of the system plus the aileron actuator.

$$\begin{cases} \mathbf{M}_A\ddot{\mathbf{q}}_a + \mathbf{C}_A\dot{\mathbf{q}}_a + \left[\mathbf{K}_A + \mathbf{\Phi}_A^T \begin{bmatrix} 0 \\ \vdots \\ 1 \\ \vdots \\ 0 \end{bmatrix} K_{act}[0 \cdots 1 \cdots 0]\mathbf{\Phi}_A\right]\mathbf{q}_a - \mathbf{\Phi}_A^T \begin{bmatrix} 0 \\ \vdots \\ 1 \\ \vdots \\ 0 \end{bmatrix} K_{act}\,\delta_0 = \mathbf{0} \\ \ddot{\delta}_0 + 2\xi\omega_n\dot{\delta}_0 + \omega_n^2\delta_0 = \omega_n^2\delta_{c_{ail}} \end{cases}$$

Such system can be solves sequentially, by first solving the bottom equation in terms of δ_0 and then use the solution as the forcing term in the top equation. An alternative option is to exploit a state space formulation with the following matrices, state vector and input:

$$\begin{cases} \dot{\mathbf{x}} = \mathbf{A}\mathbf{x} + \mathbf{B}\mathbf{u} \\ \mathbf{y} = \mathbf{C}\mathbf{x} + \mathbf{D}\mathbf{u} \end{cases}$$

$$\mathbf{A} = \begin{bmatrix} \mathbf{0} & \mathbb{I} \\ -\mathbf{M}_A^{-1}\mathbf{K}_A & -\mathbf{M}_A^{-1}\mathbf{C}_A \end{bmatrix} \qquad \mathbf{B} = \omega_n^2 \begin{bmatrix} 0 \\ \vdots \\ 0 \\ 1 \\ 0 \\ \vdots \\ 0 \end{bmatrix} \qquad \mathbf{C} = [0 \cdots 0\,1\,0 \cdots 0] \qquad \mathbf{D} = 0$$

$$\mathbf{x} = \begin{bmatrix} \mathbf{q}_a \\ \dot{\mathbf{q}}_a \\ \delta_0 \\ \dot{\delta}_0 \end{bmatrix} \qquad \mathbf{u} = \delta_{c_{ail}}$$

Task 2: Adding rotor actuator

The rotor actuator presents the same dynamics of the aileron stiffness with the slight difference that the stiffness is imposed to be $K_{act} = 1 \cdot 10^8 {}^{Nm}/_{rad}$.

By repeating the same steps, we are able to build a similar system of equations, with the slight difference that in this case we are going to have four different control inputs (one for each actuator) and four actuator dynamics equations. Therefore:

$$\begin{cases} \mathbf{M}_A\ddot{\mathbf{q}}_a + \mathbf{C}_A\dot{\mathbf{q}}_a + \left[\mathbf{K}_A + \sum_{i=0}^{3} \mathbf{\Phi}_A^T \begin{bmatrix} 0 \\ \vdots \\ 1 \\ \vdots \\ 0 \end{bmatrix} K_{act_i} [0 \cdots 1 \cdots 0] \mathbf{\Phi}_A \right] \mathbf{q}_a - \sum_{i=0}^{3} \mathbf{\Phi}_A^T \begin{bmatrix} 0 \\ \vdots \\ 1 \\ \vdots \\ 0 \end{bmatrix} K_{act_i}\, \delta_i = \mathbf{0} \\ \ddot{\delta}_0 + 2\xi\omega_n\dot{\delta}_0 + \omega_n^2\delta_0 = \omega_n^2\delta_{c_{ail}} \\ \ddot{\delta}_1 + 2\xi\omega_n\dot{\delta}_1 + \omega_n^2\delta_1 = \omega_n^2\delta_{c_{rot_1}} \\ \ddot{\delta}_2 + 2\xi\omega_n\dot{\delta}_2 + \omega_n^2\delta_2 = \omega_n^2\delta_{c_{rot_2}} \\ \ddot{\delta}_3 + 2\xi\omega_n\dot{\delta}_3 + \omega_n^2\delta_3 = \omega_n^2\delta_{c_{rot_3}} \end{cases}$$

Once again, such system can be solved sequentially, by first solving the bottom equations in terms of δ_0, δ_1, δ_2 and δ_3 and then use the solution as the forcing term in the top equation. An alternative option is to exploit a state space formulation with the following matrices, state vector and input:

$$\begin{cases} \dot{\mathbf{x}} = \mathbf{A}\mathbf{x} + \mathbf{B}\mathbf{u} \\ \mathbf{y} = \mathbf{C}\mathbf{x} + \mathbf{D}\mathbf{u} \end{cases}$$

$$\mathbf{A} = \begin{bmatrix} \mathbf{0} & \mathbb{I} \\ -\mathbf{M}_A^{-1}\mathbf{K}_A & -\mathbf{M}_A^{-1}\mathbf{C}_A \end{bmatrix} \qquad \mathbf{B} = \omega_n^2 \begin{bmatrix} 0 & 0 & 0 & 0 \\ & & \vdots & \\ 1 & 0 & 0 & 0 \\ 0 & 1 & 0 & 0 \\ 0 & 0 & 1 & 0 \\ 0 & 0 & 0 & 1 \\ 0 & 0 & 0 & 0 \\ 0 & 0 & 0 & 0 \\ 0 & 0 & 0 & 0 \\ 0 & 0 & 0 & 0 \end{bmatrix} \qquad \mathbf{C} = [0 \cdots 0\,1\,0 \cdots 0] \qquad \mathbf{D} = 0$$

$$\mathbf{x} = \begin{bmatrix} \mathbf{q}_a \\ \dot{\mathbf{q}}_a \\ \delta_0 \\ \delta_1 \\ \delta_2 \\ \delta_3 \\ \dot{\delta}_0 \\ \dot{\delta}_1 \\ \dot{\delta}_2 \\ \dot{\delta}_3 \end{bmatrix} \qquad \mathbf{u} = \begin{bmatrix} \delta_{c_{ail}} \\ \delta_{c_{rot_1}} \\ \delta_{c_{rot_2}} \\ \delta_{c_{rot_3}} \end{bmatrix}$$

Task 3: Flutter test and flutter control

To simulate the flutter test, the system was perturbed at various airspeeds with the use of the aileron actuator excited with frequency sweeps and frequency dwells input signals. This is a common practice in the aerospace industry for different reasons. Firstly, by perturbing the system at different frequencies, we are able to assess at what frequency the system reacts the most, thereby locating the modes with lowest damping and thus more prone to instabilities. This approach also allows us to use the logarithmic decrement method to experimentally estimate the damping ratio of a mode. Secondly, with this practice, a greater level of safety is ensured as we are forcing a response of a system near flutter conditions rather than approaching flutter, thus the disturbance amplitude can be carefully controlled and terminated if necessary.

From Figure 3 which shows the eigenfrequency and damping ratio as a function of airspeed, mode 8 becomes unstable around 200 m/s. For this reason, the airspeed used to simulate the flutter test is 189.2 m/s as the system is still stable but with a low damping ratio on the critical mode.

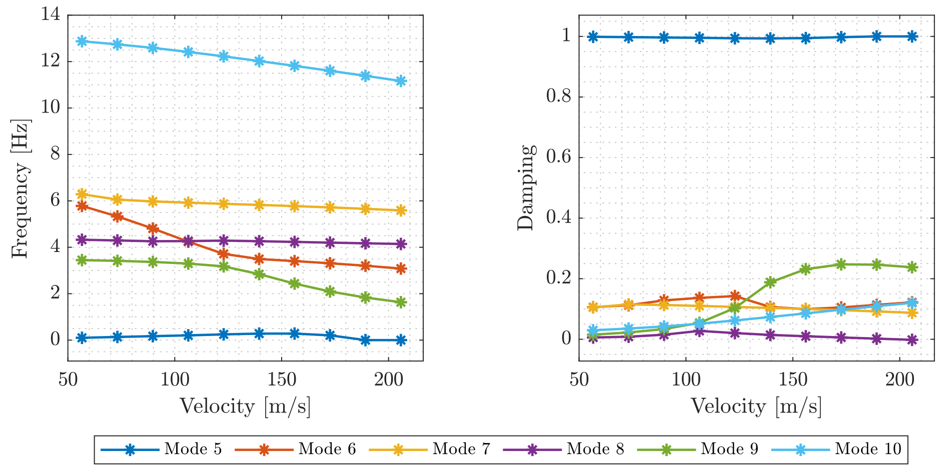

Figure 2: TBD

Remark: Based on previous workshops, the structural mode associated with whirl flutter is identified as an out-of-plane bending mode. Therefore, it is reasonable to excite the system using the aileron rather than employing cyclic or collective pitch excitation from the rotor.

The procedure to evaluate the flutter response is as follows. First we applied the frequency sweep in order to observe the characteristic frequencies of the aeroelastic system. This was done using the MATLAB function `chirp( )`, with an amplitude of 0.2 *rad* as demanded in the task, and with a frequency rage of 0.1 Hz to 8 Hz. The lower end was chosen based on a trial and error procedure while the higher end was selected based on maximum actuator frequency (as seen by the bode plot of the actuator dynamics in Figure 1). The flutter analysis was then carried out as usual with the continuation approach. As shown in Figure 3, the system's response reaches its highest amplitude at a frequency of 4.535 Hz. That is to be considered the frequency of the lowest damped mode.

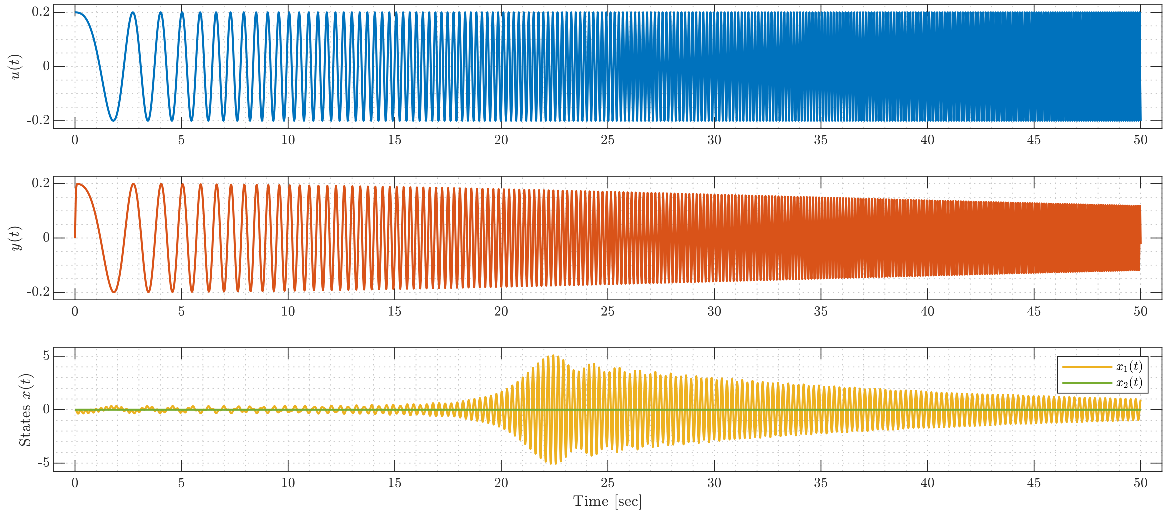

Figure 3: Frequency sweep response

Remark: From figure 3 two things can be noted. Firstly, the trend of the response $y(t)$ - aileron deflection - with respect to frequency, confirms that the choice of the upper frequency bound (8 Hz) was right. In fact, this amplitude deviates from the input one $u(t)$ when increasing the frequency. Secondly, the states plot underlines that, independently on the state that we are taking into account, the maximum amplitude occurs at the same frequency, that is the frequency of the 8th mode. The difference in the amplitude that can be noticed between state $x_1(t)$ and $x_2(t)$, is due to the fact that the first state- rigid aileron movement - is more coupled with the out-of-plane bending flutter mode than the second state - rigid swash plate movement -.

Once the characteristic frequencies were evaluated, we proceeded with the analysis of the response of the system to constant frequency (4.535 Hz) and amplitude command inputs (frequency dwells). This analysis allows to excite the system to a specific frequency and once the excitation is stopped, assess the logarithmic decrement of the system. In this case, because we are exiting at the frequency of the lowest damped mode, we are going to observe the logarithmic decrement associated with the lowest damped mode. In Figure 4 we can observe two regions of the response: the initial transient and the logarithmic decrement once the excitation is stopped.

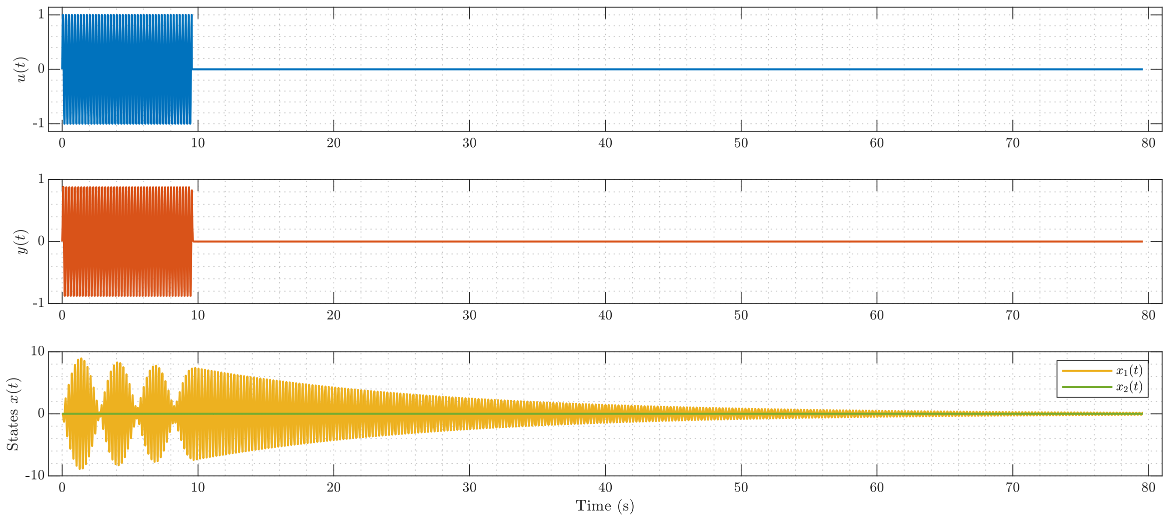

Figure 4: Frequency dwell response

Finally, by extracting the last part of the response and applying the logarithmic decrement method, we are able to compute the damping ratio. Given the fact that the peaks are bounded by a logarithmic decrement, each peak decreases by a damped exponential term:

$$x(t+T) = x(t)e^{-\xi\omega_n T}$$

Therefore, by computing the quantity $\delta = \ln\left(\frac{x(t)}{x(t+T)}\right)$, and recalling that: Since:

$$\delta = \xi\omega_n T \qquad T = \frac{2\pi}{\omega_d} \qquad \omega_n = \frac{\omega_d}{\sqrt{1-\xi^2}}$$

We can easily write:

$$\delta = \xi\frac{2\pi}{\sqrt{1-\xi^2}} \qquad \Longrightarrow \qquad \xi = \frac{\delta}{\sqrt{\delta^2+4\pi^2}}$$

In our case, the logarithmic decrement consisted of multiple peaks. Therefore, we calculated a δ ratio for each peak pair and then determined the mean value. The computed damping ratio was $\xi = 0.002067$. In Figure 5 it can been seen more clearly the portion of the response used in the logarithmic decrement calculation.

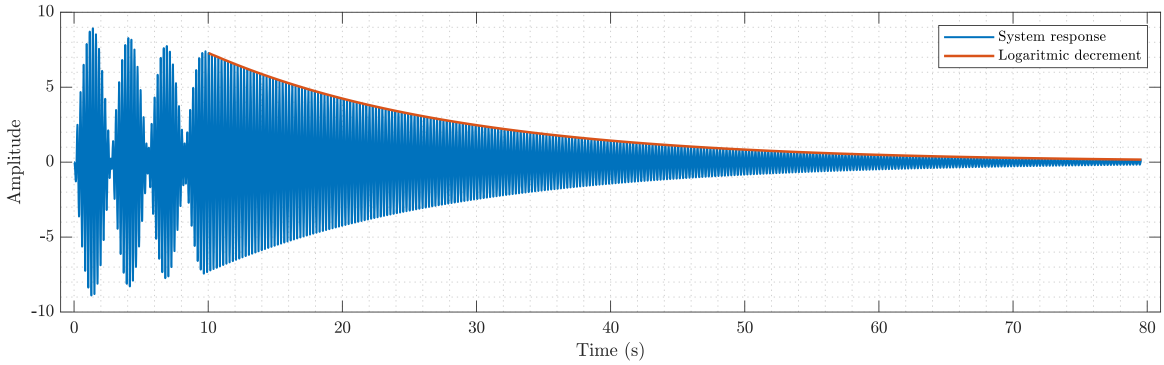

Figure 5: Logarithmic decrement

Remark: The lowest damped mode can be identified with the 8$^{\text{th}}$ mode and exhibits a soft flutter behavior. It is important to note that in this case with respect to the previous workshop, the aircraft does not fully enter flutter. The presence of gimbal modes prevents a true flutter condition, although the damping remains extremely low, indicating a marginally stable system.

Remark: It is interesting to note that the frequency and damping obtained from the eigenanalysis and those derived from the logarithmic decrement analysis show minimal discrepancies. The eigenanalysis produced a frequency of 4.3248 Hz with a damping ratio of $\xi = 0.002067$, while the logarithmic decrement analysis determined a frequency of 4.5351 Hz with the same damping ratio. Both results were computed at an airspeed of 189.2 $^{\text{m}}/_{\text{s}}$, demonstrating consistency in damping predictions despite minor frequency variations.

Work partition

The workshop was carried out in full cooperation between the team members. The codes of all tasks were developed and cross-checked together as well as the drafting of the report. For this reason it is not possible to allocate the single contributions of each team member.